



Distinct microalgae species for food—part 1: a methodological (top-down) approach for the life cycle assessment of microalgae cultivation in tubular photobioreactors

S. Schade¹ · T. Meier^{1,2}

Received: 8 January 2020 / Revised and accepted: 5 June 2020 / Published online: 7 July 2020
© The Author(s) 2020

Abstract

Specific microalgae species are an adequate source of EPA and DHA and are able to provide a complete protein, which makes them highly interesting for human nutrition. However, microalgae cultivation has also been described to be energy intensive and environmentally unfavorable in pilot-scale reactors. Moreover, production in cold temperature zones has not been sufficiently investigated. In particular, the effects of tube materials and cultivation season length have rarely been previously investigated in the context of a comparative LCA of microalgae cultivation. A computational “top-down” model was conducted to calculate input flows for *Nannochloropsis* sp. and *Phaeodactylum tricornutum* cultivation in a hypothetical tubular photobioreactor. Cultivation processes were calculated according to detailed satellite climatic data for the chosen location in Central Germany. This model was applied to a set of different scenarios, including variations in photobioreactor material, tube diameter, microalgae species, and cultivation season length. Based on these data, a life cycle assessment (LCA) was performed following ISO standard 14040/44. The impact assessment comprised the global warming potential, acidification, eutrophication, cumulative energy demand, and water scarcity. The results showed that a long cultivation season in spring and fall was always preferable in terms of environmental impacts, although productivity decreased significantly due to the climatic preconditions. Acrylic glass as a tube material had higher environmental impacts than all other scenarios. The cultivation of an alternative microalgae species showed only marginal differences in the environmental impacts compared with the baseline scenario. Critical processes in all scenarios included the usage of hydrogen peroxide for the cleaning of the tubes, nitrogen fertilizer, and electricity for mixing, centrifugation, and drying. Microalgae cultivation in a tubular photobioreactor in a “cold-weather” climate for food is sustainable and could possibly be a complement to nutrients from other food groups. The added value of this study lies in the detailed description of a complex and flexible microalgae cultivation model. The new model introduced in this study can be applied to numerous other scenarios to evaluate photoautotrophic microalgae cultivation in tubular photobioreactors. Thus, it is possible to vary the facility location, seasons, scale, tube dimensions and material, microalgae species, nutrient inputs, and flow velocity. Moreover, single processes can easily be complemented or exchanged to further adjust the model individually, if, for instance, another downstream pathway is required.

Keywords Microalgae cultivation · LCA · Global warming · Environmental impacts · *Nannochloropsis* sp. · Photobioreactor · PBR

Electronic supplementary material The online version of this article (<https://doi.org/10.1007/s10811-020-02177-2>) contains supplementary material, which is available to authorized users.

✉ S. Schade
susann.schade@landw.uni-halle.de

¹ Institute for Agricultural and Nutritional Sciences, Martin Luther University Halle-Wittenberg, Von-Danckelmann-Platz 2, 06120 Halle, Germany

² Competence Cluster for Nutrition and Cardiovascular Health (nutriCARD), Jena-Halle-Leipzig, Germany

Introduction

The nutritional supply for a growing world population has been widely discussed in the literature, where possible solutions to meet the increasing food demands include a shift in diet patterns toward plant-based options, further development of technologies, reduction in food waste, land expansion, and yield enhancement (Cazcarro et al. 2019). In this context, other food sources have increasingly gained interest to provide sufficient nutrients for humans globally, including cultured meat, insects, and macro- and microalgae (Parodi et al. 2018).

Microalgae have the potential to provide crucial nutrients for human nutrition, such as vitamins including B₁₂, sterols, polysaccharides, carotenoids, dietary fiber, and antioxidants (Mišurcová et al. 2012; Wells et al. 2017; Borowitzka 2018). Relevant microalgae species can contain high percentages of protein, including all essential amino acids (Safi et al. 2014; Gutiérrez-Salmeán et al. 2015), which could be a decent complement to more conventional high-impact protein sources such as meat and dairy products, especially since it is estimated that approximately 1 billion people today have deficient protein intake (Caporgno and Mathys 2018). Another promising characteristic of some microalgae species is their elevated content of polyunsaturated fatty acids (PUFAs), particularly eicosapentaenoic acid (EPA) and docosahexaenoic acid (DHA), which are otherwise only found in seafood. Oleaginous microalgae such as *Nannochloropsis* sp. could thus help reduce excessive pressure on the fish market.

The photoautotrophic cultivation of microalgae largely depends on solar insolation and temperature. The outdoor location of cultivation systems has been preferred to avoid exorbitant costs for radiation and temperature control. A great part of microalgae that are cultivated for human nutrition today are produced in open raceway ponds (ORPs) located in Asia. Large plants also operate in Australia and Israel (Borowitzka 2013). However, the evaluation of microalgae cultivation in different geographical and climatic locations is crucial to exploit their true potential in providing nutrients for humans globally. In particular, cultivation in cold areas of temperate climatic zones has only been investigated in a few studies (Pérez-López et al. 2017; Smetana et al. 2017). A previous study by Schade and Meier (2019) suggested that photobioreactors (PBRs) are the most suitable for production in cold climates. Moreover, *Nannochloropsis* sp. has been reported to be easily contaminated with bacteria, other microalgae, or protozoa and is therefore best suited to closed cultivation systems (Rocha et al. 2003). Furthermore, PBRs are described to enable a higher photosynthetic efficiency than ORPs and thus also a higher productivity. PBRs use less water due to the absence of evaporation, and they allow more precise management of ambient conditions (Enzing et al. 2014; Huang et al. 2017), which is of high interest for the cultivation of microalgae for food. In contrast, most of the life cycle assessments (LCAs) on microalgae so far have focused on the usage of microalgae as some form of bioenergy. Not only do functional units and system boundaries differ from the methodological settings of food LCAs, but also cultivation standards cannot be guaranteed to be congruent with those used for the production of food.

Precise data on the industrial-scale cultivation of microalgae for food, especially in PBRs, are still scarce. Moreover, former analyses tended to extrapolate data from laboratory- and pilot-scale cultivation plants to obtain relevant

input flows, thus using a methodological “bottom-up” approach (Lardon et al. 2009; Collet et al. 2014; Keller et al. 2017; Smetana et al. 2017). The present study relies on the cultivation of the microalgae species *Nannochloropsis* sp. in a hypothetical tubular PBR in Central Germany as an example of a “cold-weather” temperate climate. Productivity is calculated after a 4-year average of location-specific satellite data using the NASA Power Data Access Viewer (NASA—National Aeronautics and Space Administration 2019). The location-specific data are used in a set of calculations to conduct a life cycle inventory following a “top-down” approach. Subsequently, the environmental impacts of microalgae cultivation are investigated using LCA following ISO standard 14040/44 (ISO Organization 2006).

The strength of the study lies in the complex and flexible microalgae cultivation model, which can be applied to multiple other scenarios to evaluate microalgae cultivation in tubular PBRs. Thus, it is possible to vary the facility location, seasons, scale, tube dimensions and material, microalgae species, nutrient inputs, and flow velocity. Moreover, single processes can easily be complemented or exchanged to further adjust the model individually, if, for instance, another downstream pathway is required.

This is the first part of a two-part study to analyze the environmental impacts of industrial scale microalgae cultivation in photobioreactors in a “cold-weather” climate. Part 2 of the study (Schade et al. 2020) is a comparative life cycle assessment that uses relevant scenarios of part 1 as well as additional scenarios and compares the environmental impacts of microalgae in a “cold-weather” climate to those from different fish products based on the nutritional value of the products. The implementation of microalgae as a source of essential nutrients is extensively discussed, and their significance for food is evaluated.

Materials and methods

LCA framework

Goal and scope

The objective of the study was to assess the environmental impacts of generic industrial-scale microalgae production for food in a horizontally stacked tubular PBR in Germany. To meet this objective, this study aimed to develop a computational model for the calculations of relevant input flows during microalgae cultivation. Furthermore, different scenarios for the cultivation of microalgae were tested comprising variations in reactor design, the choice of microalgae species, and different cultivation season lengths due to climatic preconditions. More specifically, the scenarios differed in the choice of tube material, as borosilicate glass and polymethyl

methacrylate (PMMA) were used. Concerning the borosilicate glass scenarios, two different tube diameters were tested, namely, 40 mm and 36 mm. For the PMMA tubes, two different lifespans of 3 and 7 years (with reduced productivity) were assumed. The microalgae species *Nannochloropsis* sp. and *Phaeodactylum tricornutum* were assessed to test possible variations due to the microalgae species. For each of the scenarios, three different cultivation season lengths were applied.

Modeling approach

An attributional modeling approach was chosen with allocation “at the point of substitution,” as it was considered the most accurate for the application of waste treatment. Carbon sequestration during cultivation was modeled as an avoided burden. Waste treatment, including recycling, was modeled for all reactor materials.

System boundaries

The system boundaries comprised all processes up to the dry microalgae biomass. An overview of the system boundaries is given in Fig. 1. As microalgae production for food was assessed, the whole dry biomass as the target product was assumed most appropriate given that microalgae are commonly sold in this form as supplements. Similar system boundaries have rarely been used in preceding studies (Taelman et al. 2013; Zaimes and Khanna 2013; Pérez-López et al. 2017).

In contrast, many studies relied on different kinds of downstream processing included in the system boundaries (Lardon et al. 2009; Batan et al. 2010; Campbell et al. 2011; Khoo et al. 2011; Yanfen et al. 2012; Soratana et al. 2013; Collet et al. 2014; Pérez-López et al. 2014; Quinn et al. 2014; Bennion et al. 2015; Silva et al. 2015; Wu et al. 2017; Smetana et al. 2017).

Functional unit

For both the methodological calculations and the compilation of the life cycle inventory, 1-kg DM (dry mass) was used as the functional unit for microalgae, as dry biomass was chosen to be the final product in this study. Previous studies often included the use of an energetic functional unit in correlation with the assessment of microalgae for energy or biofuels (Collet et al. 2011; Hou et al. 2011; Khoo et al. 2011; Yanfen et al. 2012; Grierson et al. 2013; Taelman et al. 2013; Zaimes and Khanna 2013; Woertz et al. 2014; Monari et al. 2016; Wu et al. 2017; Raghuvanshi et al. 2018). Occasionally, mass-based functional units corresponding to a certain ingredient have been used, such as lipids or astaxanthin (Pérez-López et al. 2014; Keller et al. 2017; Collotta et al. 2018). The mass-based functional unit in this study was considered most appropriate given that groceries commonly rely on 1 kg or 100 g to indicate ingredients and nutrient contents.

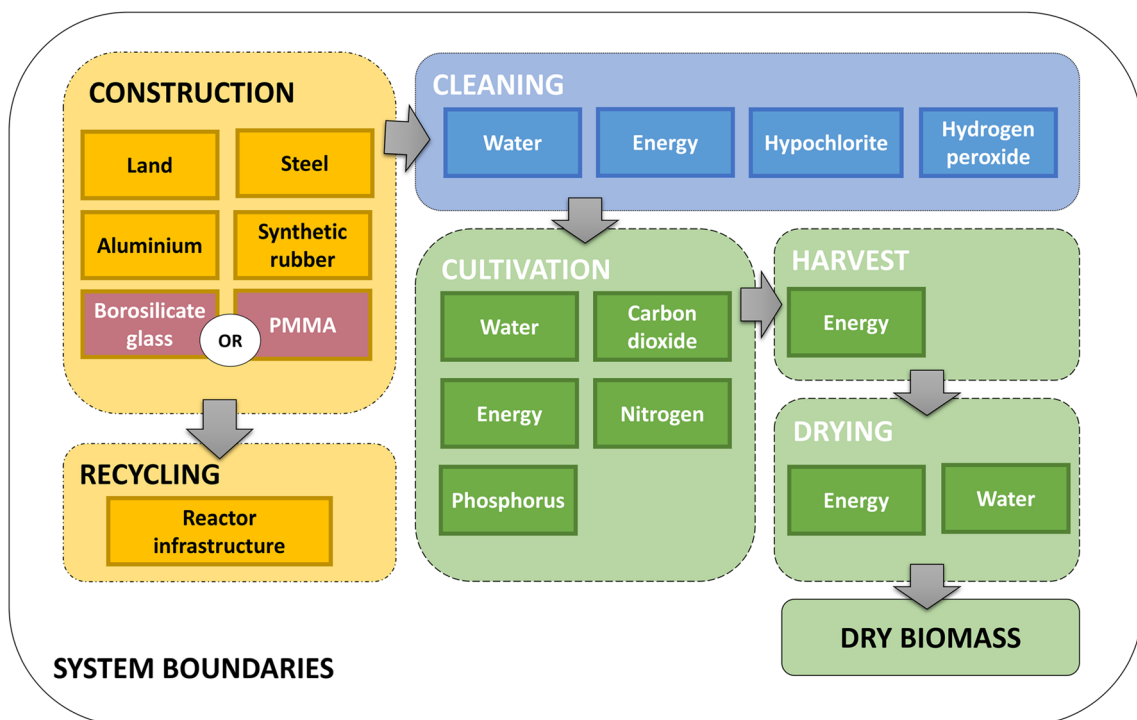


Fig. 1 System boundaries of microalgae cultivation in a tubular PBR

Data source

A combination of different resources was relied on for the foreground data. Foreground data were partly acquired from the literature and supplemented with information gained through expert interviews. Data derived from the literature comprised the nutritional composition of the microalgae species used, the photoconversion efficiency (PCE), nutrient inputs during cultivation, cleaning substances, materials for the supporting structures of the PBR, and flow velocity in the PBR. Detailed references are given in “System design of microalgae cultivation” section. Detailed climatic data were obtained from the NASA Data Access Viewer (NASA—National Aeronautics and Space Administration 2019). To assess the relevant input flows for the conduction of the LCA, the selected data were drawn from our own calculations. The Ecoinvent v3.4 “APOS” system model (“allocation at the point of substitution”) was used for the calculation of all background processes (Wernet et al. 2016).

Life cycle impact assessment

For the life cycle impact assessment (LCIA) of the microalgae scenarios, global warming potential was quantified and expressed as CO₂eq according to IPCC 2013 GWP 100a (IPCC 2014). Acidification and eutrophication were recorded as SO₂eq and PO₄⁻eq based on CML-IA Baseline EU25 (de Bruijn et al. 2002). The calculation of the cumulative energy demand was based on the method published by Ecoinvent v2 and expanded by PRé Consultants (Frischknecht et al. 2007). To assess blue water use, different methods were applied. Water scarcity was analyzed using AWARE (Boulay et al. 2018) and the water stress index according to Hoekstra et al. 2012 (Hoekstra et al. 2012). Additionally, the values for water use conducted in the life cycle inventory (LCI) (Table S3) were analyzed according to cultivation stage.

Data quality analysis

A combination of methods was used to analyze the data quality. First, sensitivity analysis was carried out by assessing different microalgae cultivation scenarios. In the second step, Monte Carlo analysis was performed using IPCC 2013 GWP 100a in SimaPro (PRé Consultants B.V., Netherlands, version 8.5) to evaluate the variation in the results during the comparison of different scenarios. The background processes in SimaPro were supplied with a distribution factor. Concerning the foreground processes, Pedigree matrices were conducted in SimaPro using a lognormal distribution.

System design of microalgae cultivation

Geographical setting

Central Germany was chosen as the geographical setting, more specifically the city of Halle/Saale, which is located in the temperate climatic zone and shows suitable climatic pre-conditions for the cultivation of microalgae. The maximum, minimum, and mean temperatures at 2 m in °C and all sky insolation incidents on a horizontal surface in MJ m⁻² day⁻¹ were evaluated as the key parameters for microalgae cultivation. The temperature was analyzed in detail for the years 2015–2018 to identify the months that were suitable for microalgae cultivation. Insolation data were used for the calculation of yield and productivity. A further description of the method is given in “LCI processes: methodological approach” section. Moreover, the minimum and maximum wind speeds were examined and excluded from further calculation because the maximum wind speed was too low to have a cooling effect on the PBR. The same was found for precipitation rates. The climatic investigations were based on detailed monthly satellite data obtained from the NASA Power Data Access Viewer (NASA—National Aeronautics and Space Administration 2019) for the years 2015–2018, and a 4-year average was used for the calculations. The average maximum temperature reaches a peak in August at 26.2 °C. Solar insolation can reach 18.2 MJ m⁻² day⁻¹ on average in June. Detailed climatic data can be accessed in the supplementary material (Figs. S1–S2, Tables S1–S2).

Microalgae species

Nannochloropsis sp. was chosen for cultivation in the hypothetical industrial-scale tubular PBR. This species was considered due to its relatively high total lipid and protein contents. However, the values for the nutrient content ranged drastically across the literature which can be due to a great number of varying parameters, such as nutrient inputs and climatic characteristics.

The protein content of *Nannochloropsis* sp. was specified to range between 25 and 36% of DM with most studies suggesting a value of approximately 30% (Reboloso-Fuentes et al. 2001; Fábregas et al. 2004; Kent et al. 2015; Paes et al. 2016; Molino et al. 2018) which was also used in this study. Hulatt et al. (2017) described a value of 50–55% of DM during nutrient-replete conditions.

Concerning the total lipid content, the values fluctuated vastly from 5 to 44% of DM under light-saturated, non-stressed conditions with an EPA content between 1.1 and 7.48% of DM (Reboloso-Fuentes et al. 2001; Fábregas et al. 2004; Kent et al. 2015; Ma et al. 2016; Paes et al. 2016; Hulatt et al. 2017; Molino et al. 2018). These values

resulted in mean lipid and EPA contents of 20.6% and 4.2%, respectively, of DM.

To calculate the nutritional energy value, the mean carbohydrate content was taken from the literature. The carbohydrate content of *Nannochloropsis* sp. ranged between 20 and 37.6% across the studies (Reboloso-Fuentes et al. 2001; Fábregas et al. 2004; Paes et al. 2016; Molino et al. 2018) resulting in a mean value of 29%. The mean values of the macronutrients contained in *Nannochloropsis* sp. were used to calculate a nutritional energy value of 17.66 MJ kg⁻¹. This result is in accordance with the nutritional energy values in the literature, which were between 16.8 and 25.7 MJ kg⁻¹ (Reboloso-Fuentes et al. 2001; Sukarni et al. 2014; Hulatt et al. 2017).

Khatoon et al. (2014) described a salinity of approximately 30 g L⁻¹ as optimal, which was, on average, confirmed by other studies (Gu et al. 2012; Bartley et al. 2014; Ma et al. 2016).

Biomass growth and composition reached a peak at a pH between 7.5 and 9.0 (Bartley et al. 2014; Khatoon et al. 2014; Kent et al. 2015; Ma et al. 2016; Paes et al. 2016) resulting in an average pH of 8.3. Moreover, a temperature of 21 to 25 °C has been reported to enable the maximum growth rate (Chini Zittelli et al. 1999; Ma et al. 2016). The maximum cell density reaches 4.7 g L⁻¹ (Hulatt et al. 2017).

As a second scenario, *Phaeodactylum tricorutum* was cultivated in a glass tube PBR. Similar to *Nannochloropsis* sp., this microalga is characterized by reasonably high protein and lipid contents as well as a favorable fatty acid profile. The protein content can reach 36.4% of DM while the total lipid content reaches 18% on average (Reboloso-Fuentes et al. 2007). The content of EPA fluctuated between 1.10 and 5.11% of DM, and the values for DHA ranged between 0.15 and 0.13% of DM (Zhukova and Aizdaicher 1995; Ryckebosch et al. 2014). Thus, EPA and DHA contents of 3.11 and 0.14%, respectively, of DM were assumed. Based on the macronutrient profile, a nutritional energy value of 17.25 MJ kg⁻¹ was calculated. The optimum cultivation temperature was described to be approximately 20 °C, with a favorable pH of 7.7 (Silva Benavides et al. 2013).

LCI processes: methodological approach

Yield and productivity The yield is usually calculated in a “top-down” manner from the solar radiation rather than conducting extrapolations from the lab scale. In terms of autotrophic microalgae, it is commonly known that light is the primary limiting factor. To cultivate microalgae on a large scale, sunlight should be used to avoid extreme costs due to energy use. The productivity of autotrophic microalgae cultivation hence highly depends on the solar radiation of a location. Another factor determining

productivity is the photoconversion efficiency (PCE), which depends on the energy embodied in the microalgae biomass and the irradiation flux. The maximum possible solar energy converted to biomass has been described to be 10% (Lundquist et al. 2010). A PCE of 5% on average is described to be optimistic for a biomass energy value of 20 MJ kg⁻¹ dry weight (Posten 2012; Skarka 2012), whereas other studies indicate a maximum PCE of only 1 to 3% after inclusion of all constraining effects, namely, light saturation and photoinhibition as well as practical losses through reflection, inactive absorption, respiration and high oxygen rates (Lundquist et al. 2010; Benemann 2013). De Vree et al. (2015) described the photosynthetic efficiency in vertical photobioreactors to be high, ranging between 2.4 and 4.2% (De Vree et al. 2015). On average, the data obtained from the literature result in a mean PCE value of 3.4%. Thus, in this study, a constant PCE of 3.4% was assumed for the calculation of the expected yields. Equation 1 is the equation used for the calculation of the yield in kg m⁻² year⁻¹ which has been adapted from (Skarka 2012).

$$Y_a = \frac{PCE}{H_0} \sum_{m=1}^{12} \left(\prod_T I_{T,m} \times G_m \right) \quad (1)$$

- Y_a yield, in kg m⁻² year⁻¹
- PCE photoconversion efficiency, here 3.4%; 3.3% (for the PMMA 7 years scenario)
- H_0 nutritional energy value of the biomass in MJ kg⁻¹; 17.66 MJ kg⁻¹ for *Nannochloropsis* sp. and 17.25 MJ kg⁻¹ for *P. tricorutum*
- $I_{T,m}$ different temperature indicators $\in \{0;1\}$ for month m with $I_{T,m} = 1$ for a suitable month for microalgae cultivation and $I_{T,m} = 0$ for an unsuitable month
- G_m total radiation in month m in MJ m⁻²

A month was assumed to be suitable for microalgae cultivation when the mean temperature was between 0 and 35 °C, whereas the minimum temperature must not fall below 0 °C and the maximum temperature must not exceed 45 °C on more than 5 days of that month (Skarka 2012). Following this hypothesis and according to the climatic data (see supplementary material), production would be feasible from April until October. The climatic data were evaluated for the years 2015–2018. In October, the temperature usually did not fall below 0 °C. In April, the temperature was slightly below 0 °C on 2 to 5 days of the month. Accordingly, three different scenarios for the yield calculation were assumed. In the optimistic scenario, it was assumed that the whole months of April and October were suitable for cultivation. Production hence took place from April 1 until October 31 with 214 production days and a yield of 5.92 kg m⁻² year⁻¹ whereas 1 year a

always comprises the total number of production days. In contrast, the pessimistic scenario assumed that production in April and October was not feasible, and only 153 production days generated a yield of $4.78 \text{ kg m}^{-2} \text{ year}^{-1}$. Production thus took place from May 1 until September 30. An intermediate scenario was added to account for these temperature differences between years and assumed production during half the months of April and October resulting in 183 days (from April 15 until October 15) and a yield of $5.35 \text{ kg m}^{-2} \text{ year}^{-1}$.

The productivity Z_t was calculated from the values for the yield according to Eq. 2. The hypothetical facility comprises a 500-km long tube system over an area of 1.2 ha. The tubes have a diameter of 40 mm, which gives a total production volume of 628,000 L and thus a facility volume V_A of either 52.33 L m^{-2} or 42.42 L m^{-2} for 36-mm tubes.

$$Z_t = \frac{Y_a \times 1000}{t_d \times V_A} \quad (2)$$

Z_t productivity for the number of production days t , in $\text{g L}^{-1} \text{ days}^{-1}$

Y_a annual yield for the number of production days t , in $\text{kg m}^{-2} \text{ year}^{-1}$

t_d number of production days

V_A facility volume per area, here 52.33 L m^{-2} and 42.42 L m^{-2}

Infrastructure The horizontally stacked PBR consists of tubes and corners made of borosilicate glass with a lifespan of 50 years. The tubes each have a length of 100 m, a diameter of 40 mm, and a wall thickness of 2.0 mm. For further construction and supporting structures, aluminum, steel, and synthetic rubber are used (Pérez-López et al. 2017). Whereas aluminum and steel are also assumed to have a lifespan of 50 years, synthetic rubber is replaced after 10 years.

Alternatively, another borosilicate glass scenario was calculated with a tube diameter of 36 mm, while the wall thickness and PCE remained the same. This scenario is supported by the assumption that despite the diameter being diminished, the biomass concentration in the suspension will increase. While the areal productivity remains unchanged, the volumetric productivity increases, and electrical requirements as well as water use are expected to decline.

As a third scenario, the tubes were assumed to be made of acrylic glass, more specifically polymethyl methacrylate (PMMA) with opaque corners made of polypropylene (PP), while the supporting structure remained the same. PMMA is described as a potential PBR material in the literature (Burgess and Fernández-Velasco 2007; Posten 2012) and has been used in pilot-scale PBRs (Pérez-López et al. 2017). Similar to borosilicate glass, PMMA has a high transmission of over 90%

(Schultz and Wintersteller 2016). The acrylic glass tubes have the same measurements as the borosilicate glass tubes. However, the translucence of PMMA worsens by approximately 0.7% per year under full sun exposure (Schultz and Wintersteller 2016). Consequently, it was assumed that the PMMA tubes and PP corners needed to be replaced every 3 years to retain cultivation productivity and were subsequently recycled. PMMA is depolymerized to MMA through pyrolysis and can be reused (Kaminsky and Eger 2001; Perugini et al. 2005).

In an additional scenario, the acrylic tubes are maintained for 7 years and subsequently recycled. In this scenario set, a reduced PCE was assumed to account for the translucence loss in the PMMA tubes that occurs over the years.

Nutrients The total nitrogen demand was calculated from the average protein content of the microalgae species by applying the nutrient-to-protein conversion factor k , which was adopted from Templeton and Laurens (2015) and amounts to a mean value of 4.99. Thus, 1 g of nitrogen supplied per day translates to 4.99 g of protein in biomass. Assuming a protein content of 30% in *Nannochloropsis* sp., a nitrogen input of 60 g kg^{-1} biomass would be appropriate. Nitrogen is applied as nitrate which increases the pH due to the release of OH^- ions (Safafar et al. 2016).

An N:P ratio of 20:1 has been described as optimal for biomass and protein growth and EPA accumulation (Rasdi and Qin 2015), resulting in a phosphorus input of 3 g kg^{-1} of biomass. Concerning the protein content of *P. tricornutum*, nitrogen and phosphorus supplies of 73 and 3.7 g kg^{-1} of dry biomass were applied.

The input of micronutrients was omitted because it was considered negligible for the results of the environmental assessment. Additionally, it was assumed that sufficient micronutrients were included in the pumped water.

Approximately 1.8 kg CO_2 is required to produce 1 kg of dry microalgal biomass (Chisti 2007; Patil et al. 2008; Lardon et al. 2009; Ma et al. 2016) and is directly injected as pure CO_2 to adjust the pH downwards (Reboloso-Fuentes et al. 2001; Safafar et al. 2016). The usage of CO_2 during cultivation was modeled as an avoided burden.

Water Water is needed to fill the PBR and for cleaning. It was assumed that a water supply well is available in the facility area, providing freshwater for the cultivation of the microalgae. To supply the water, energy for pumping is required. It is assumed that the complete tubular system is cleaned chemically at the beginning and at the end of every cultivation season with each cleaning using twice the amount of water in the total reactor volume. In the first rinse, the tubes are flushed with water sterilized with hypochlorite (2 mg L^{-1}) to kill any possible competing algae and protozoa (Pérez-López et al. 2017). In the second rinse, water disinfected by

3% hydrogen peroxide is pumped through the tubes (Pérez-López et al. 2017). Throughout the cultivation phase, tubes are cleaned mechanically.

Electricity

Water pumping The electricity requirement of the water pump is calculated according to Eq. 3 (Engineering ToolBox 2003a). A 10-kW pump with a flow capacity of 300 m³ h⁻¹ (Tredici et al. 2016) is used to pump the groundwater from a depth of 10 m. The pump is assumed to have an efficiency of 80% (Sills et al. 2013). Following Eq. 2, the water pump requires electricity of 0.123 MJ m⁻³.

$$E_h = \frac{\rho_w \times g \times h}{\eta_p \times 10^6} \tag{3}$$

- E_h electricity for water pumping, MJ m⁻³
- ρ_w density of water, 1000 kg m⁻³
- g acceleration of gravity, 9.81 m s⁻²
- h differential head, 10 m.
- η_p pump efficiency, 80%

Initial water heating Assuming that the water coming from the well has a temperature of 10 °C, the water subsequently needs to be heated for cultivation to an average temperature of 23 °C. To heat 1 g of liquid water by 1 °C, 4.184 J are needed. To heat 628,000 L of water for the initial filling of the tubes from 10 to 23 °C, 34,158.18 MJ are required. The 509,000 L scenario requires 27,685.53 MJ of electricity for initial heating. During the cultivation season, gray water from the heat drying process is mixed with pumped water to save water and heating costs.

Aeration Aeration is required to implement CO₂ into the microalgae suspension. The equation from Sills et al. (Eq. 4) was used to calculate the electrical power necessary for aeration (Sills et al. 2013). The values for pressure and pump efficiency were adopted from Sills et al. (2013). The specific heat capacity of CO₂ (Engineering ToolBox 2005) is related to a temperature of 300 K. The inlet temperature was set according to the optimum for the cultivation of *Nannochloropsis* sp. The electricity required for aeration amounts to 0.065 MJ kg⁻¹ CO₂.

$$E_{aer} = \frac{C_p \times T_i \times \frac{1 MJ}{1000 kJ}}{\eta_p} \left[\left(\frac{P_o}{P_i} \right)^{0.286} - 1 \right] \tag{4}$$

- E_{aer} electricity for aeration, in MJ kg⁻¹ CO₂
- C_p specific heat capacity of CO₂, 0.846 kJ (kg*K)⁻¹
- T_i inlet temperature, 297 K
- η_p pump efficiency, 85%
- P_o outlet pressure, 2 atm
- P_i inlet pressure, 1 atm

Mixing Mixing is an essential process in the PBR to distribute nutrients and CO₂ and to ensure that all cells are periodically exposed to light (Greenwell et al. 2010; Enzing et al. 2014). However, the mixing intensity needs to be adjusted precisely according to the microalgae species to be cultivated to prevent cell damage due to excessive mixing (Enzing et al. 2014). Plant operation at a minimum velocity was preferred to inhibit cell damage and reduce energy consumption. A safe flow velocity to avoid photorespiration was described to be 0.5 m s⁻¹ (Norsker et al. 2012). However, Ación Fernández et al. (2001) found that a reduction in flow velocity from 0.5 to 0.35 m s⁻¹ only slightly lowered productivity, whereas the culture at 0.17 m s⁻¹ failed to attain a steady state. Consequently, a minimum flow velocity of 0.35 m s⁻¹ was assumed for this study. To calculate the daily electricity requirement of the mixing pump, Eqs. 5, 6, 7, and 8 were used (adapted from Subramanian n.d.). The physical density of a microalgae suspension usually varies between 1.00 and 1.03 kg L⁻¹, whereby temperature and salt content have a negligible influence in the suspension (Petkov and Bratkova 1996). A mean value of 1.015 kg L⁻¹ or 1015 kg m⁻³ was used.

$$E_{mix} = \frac{p_s \times Q \times g \times h_f \times 24h \times \frac{0.001 kW}{1 W} \times \frac{3.6 MJ}{1 kWh}}{\eta_p} \tag{5}$$

- E_{mix} daily electricity input for mixing, in MJ d⁻¹
- ρ_s suspension density, 1015 kg m⁻³
- Q volumetric flow rate; 0.00043982 m³ s⁻¹ in this study for 40-mm tubes and 0.00035626 m³ s⁻¹ for 36-mm tubes
- g acceleration of gravity, 9.81 m s⁻².
- h_f head loss, 2218.203 m
- η_p pump efficiency, 85%

$$Q = \frac{\pi}{4} \times D^2 \times v \tag{6}$$

- D : tube diameter, here 0.04 m or 0.036 m.
- v : suspension velocity, here 0.35 m s⁻¹

$$h_f = 2f \times \left(\frac{L}{D} \right) \times \left(\frac{v^2}{g} \right) \tag{7}$$

- f friction factor
 L length of tube system, here 500,000 m
 D tube diameter, here 0.04 m or 0.036 m
 v suspension velocity, 0.35 m s^{-1}
 g acceleration of gravity, 9.81 m s^{-2}

The friction factor f in a turbulent flow can be calculated using the Zigrang-Sylvester equation (Eq. 8) (Subramanian). Therefore a glass roughness value of 0.0015 mm was applied (Pipe Flow Software 2019).

$$\frac{1}{\sqrt{f}} = -4 \times \log_{10} \left[\frac{\varepsilon}{3.7} - \frac{5.02}{Re} \times \log_{10} \left(\frac{\varepsilon}{3.7} + \frac{13}{Re} \right) \right] \quad (8)$$

- ε roughness value, 0.0000015 m
 D tube diameter, here 0.04 m or 0.036 m
 Re Reynolds number; 14,210 for 40-mm tubes and 12,789 for 36-mm tubes.

The Reynolds number can be calculated as follows in Eq. 9. A reasonable value for the viscosity of green and blue-green microalgae was specified between 0.9 and 1.2 mPa*s (Petkov and Bratkova 1996) which results in a mean value of 1.05 mPa*s or $0.001 \text{ kg (m}^* \text{ s)}^{-1}$. Pump efficiency was again assumed to be 85% (Sills et al. 2013). Following Eq. 8, the applied parameters result in a Reynolds number of 14,210 for the 628 m³ PBR and 12,789 for the 509 m³ PBR. A velocity with a Reynolds number of more than 2320 is described as a turbulent flow.

$$Re = \frac{\rho_s \times v \times D}{\mu} \quad (9)$$

- ρ_s suspension density, 1015 kg m^{-3}
 v suspension velocity, 0.35 m s^{-1}
 D tube diameter, here 0.04 m or 0.36 m
 μ viscosity of microalgae suspension, $0.001 \text{ kg (m}^* \text{ s)}^{-1}$

The head loss due to the binders that connect the straight circular tubes was not taken into account. It was calculated that these binders cause an additional electricity requirement of 0.01 MJ kg^{-1} dry microalgae biomass, which was considered negligible.

Harvesting: centrifugation Microalgal biomass is continuously harvested during the daytime through microfiltration and subsequent centrifugation followed by spray drying with natural gas. The average biomass concentration before entering the centrifuge was calculated to be 1.4 g L^{-1} (Al hattab et al.

2015; Olofsson et al. 2015; Pérez-López et al. 2017; Fasaei et al. 2018). The total centrifuge electricity required to produce 1 kg of microalgal slurry with 15% TSS (total suspended solids) is calculated following Eq. 10. To concentrate the microalgae suspension to approximately 15% TSS, the centrifuge uses 0.7 to 1.3 kWh m⁻³ (Greenwell et al. 2010; Grierson et al. 2013; Pahl et al. 2013; Barros et al. 2015; Fasaei et al. 2018), whereas the centrifugation works with an efficiency of approximately 95% (Pérez-López et al. 2014).

$$E_{cen} = \frac{E_{cen/m^3}}{B \times \eta_c} \times \frac{3.6 \text{ MJ}}{1 \text{ kWh}} \quad (10)$$

- E_{cen} electricity for centrifugation in MJ kg⁻¹ dry microalgae biomass
 E_{cen/m^3} electricity use of centrifuge per m³, 1.1 kWh m^{-3} .
 B average biomass concentration in suspension, 1.4 kg m^{-3}
 η_c centrifuge efficiency, 95%

After centrifugation, the remaining water is reused and thus reenters the cultivation system to decrease the environmental impacts from excessive water consumption. Therefore, energy for water pumping is required again, which is calculated using Eq. 3. This time, a differential head of 1 m is assumed to return the water to the system. To reduce the biomass concentration in the suspension from 0.0014 to 0.15 kg L⁻¹, 107 L of water must be removed by the centrifuge per kg of suspension with 15% TSS, and this water is then pumped back into the system. The total daily amount of water that needs to be pumped back is calculated by determining the amount of water that is centrifuged every day minus the daily biomass yield (Eq. 11). The absolute daily biomass yield can be determined using Eq. 12.

$$V_w = \frac{Z_d}{B} - Z_d \times \frac{1 \text{ m}^3}{1000 \text{ kg}} \quad (11)$$

- V_w volume of water for repumping, m³ day⁻¹
 Z_d absolute daily production mass, kg day⁻¹
 B average biomass concentration in suspension, here 1.4 kg m^{-3}

$$Z_d = Z_t \times V \times \frac{1 \text{ kg}}{1000 \text{ g}} \quad (12)$$

- V reactor volume; 628,000 L for 40-mm tubes and 509,000 L for 36 mm tubes

Z_t productivity for a number of production days t , in $\text{g L}^{-1} \text{d}^{-1}$.

Drying After the concentration phase through centrifugation, the microalgae slurry has a dry matter content of approximately 15% and is spray dried with natural gas. The natural gas is burned in an industrial boiler to generate heat for drying the microalgae slurry from 15% TSS to 95% TSS assuming a boiler efficiency of 75% (Zaimes and Khanna 2013). A low water content in the microalgae biomass extends the shelf life and reduces the weight for transport (Fasaei et al. 2018). The energy required to evaporate the water is calculated following Eq. 13 (Zaimes and Khanna 2013). Upon entering the boiler, the slurry is assumed to have an average temperature of 23 °C.

$$E_{dryNG} = \frac{m \times (C_w + C_v \times \Delta T)}{\eta_b} \times \frac{1 \text{ MJ}}{1000 \text{ kJ}} \quad (13)$$

E_{dryNG} heat electricity for drying from burning natural gas in a boiler, in MJ kg^{-1} dry microalgae biomass
 m mass of water needed to be extracted, in kg kg^{-1} dry microalgae biomass, 5.33 kg kg^{-1}
 C_w latent heat of evaporation of water, in kJ kg^{-1} , 2256 kJ kg^{-1} (Engineering ToolBox 2003b)
 C_v specific heat of water, in $\text{kJ kg}^{-1} \text{C}^{-1}$, 4.187 $\text{kJ kg}^{-1} \text{C}^{-1}$ (Engineering ToolBox 2003b)
 ΔT change in temperature of water, in °C, here 77 °C
 η_b boiler efficiency, 75%

It is assumed that part of the evaporated water is pumped back into the cultivation system after having been mixed with pumped water from the well to sustain the adequate cultivation temperature. Thus, 16% of the evaporated water at a temperature of 90 °C can be mixed with 84% freshly pumped water at a temperature of 10 °C to reach an adequate cultivation temperature. Consequently, 0.85 kg of evaporated water will be recycled (repumped into the system), whereas 4.48 kg of water must be freshly pumped for every kg of dry microalgae biomass harvested.

Results

Yield and productivity of microalgae cultivation scenarios

The yield and productivity of the different microalgae cultivation scenarios were assessed according to the PBR volume, the PCE, the length of the cultivation season, and the microalgae species, as shown in Table 1. Concerning the annual values, 1 year a always comprised the respective length of the cultivation season. The baseline scenario covers the

production of *Nannochloropsis* sp. in 40 mm borosilicate glass and PMMA tubes. The yield and productivity of the cultivation of *P. tricornutum* varied due to the different nutritional profiles that affected the calculations. *Phaeodactylum tricornutum* thus exhibited slightly higher values for yield and productivity than *Nannochloropsis* sp. Cultivation in 36 mm borosilicate glass tubes reduced the PBR volume from 628 to 509 m^3 due to the diminished diameter. The length of the tube system remained the same. While it was assumed that the areal productivity would be unchanged as a result of an increased biomass concentration in the medium due to the enhanced exposure to light, the volumetric productivity consequently increased considerably. Hence, the scenario comprising production in PMMA tubes for 7 years before they are recycled was characterized by the lowest values for yield and productivity. This finding resulted from the reduction in the PCE of 0.1% to portray the reduced translucence in the acrylic glass that occurs over the years of sun exposure. All scenarios showed that the shorter the length of the cultivation season was, the higher the volumetric productivity. However, the areal yield significantly decreased in all scenario sets when the cultivation season was short causing the highest total yields in the optimistic long cultivation scenarios.

Environmental impacts of microalgae cultivation

The production of microalgae dry biomass results in greenhouse gas emissions between 1.35 and 1.76 $\text{kg CO}_2\text{eq kg}^{-1}$ DM (Table 2), except for the scenarios where PMMA was used as the PBR material, which were clearly dominated by emissions from infrastructure materials. The highest value of 4.70 $\text{kg CO}_2\text{eq kg}^{-1}$ DM arose from the pessimistic PMMA scenario with a 3-year usage of acrylic glass tubes. Even though the 7-year usage of acrylic glass tubes before they are recycled reduces productivity, this set of scenarios exhibits significantly lower greenhouse gas emissions between 2.61 and 2.96 $\text{kg CO}_2\text{eq kg}^{-1}$ DM than the 3-year usage of PMMA tubes. Figure 2 shows that all scenarios profit from the use of CO_2 , which is modeled as an avoided burden and decreases the emissions from microalgae cultivation. The greatest greenhouse gas emissions are caused by hydrogen peroxide that is used at the beginning and at the end of each cultivation season to sterilize the PBR tubes. Further critical processes include nitrogen fertilizer, electricity for mixing during cultivation, and electricity for centrifugation and drying to harvest the biomass. The high greenhouse gas emissions for electricity processes mainly originate from the use of fossil energy sources. Exact values for global warming potential according to subprocesses can be found in the supplementary material for all scenarios (Table S4).

All cultivation scenarios show similar values for the eutrophication potential according to the CML IA Baseline in Fig. 3. The eutrophication potential ranges between 0.008 and

Table 1 Scenario-specific key data (yield in $\text{kg m}^{-2} \text{ year}^{-1}$ and $\text{t ha}^{-1} \text{ year}^{-1}$, productivity in $\text{g L}^{-1} \text{ day}^{-1}$)

Scenarios	Microalgae species	PBR volume in m^3	PCE in %	Production time mm/dd	Production days	Yield in $\text{kg m}^{-2} \text{ year}^{-1}$	Total yield in $\text{t ha}^{-1} \text{ year}^{-1}$	Productivity in $\text{g L}^{-1} \text{ day}^{-1}$
Baseline: 40-mm tubes	Optimistic	628	3.4	04/01–10/31	214	5.92	59.2	0.53
	Intermediate	628	3.4	04/15–10/15	183	5.35	53.5	0.56
	Pessimistic	628	3.4	05/01–09/30	153	4.78	47.8	0.60
Alternative microalgae species: <i>Phaeodactylum tricornutum</i>	Optimistic	628	3.4	04/01–10/31	214	6.07	60.7	0.54
	Intermediate	628	3.4	04/15–10/15	183	5.48	54.8	0.57
	Pessimistic	628	3.4	05/01–09/30	153	4.89	48.9	0.61
Alternative reactor design: 36 mm tubes	Optimistic	509	3.4	04/01–10/31	214	5.92	59.2	0.65
	Intermediate	509	3.4	04/15–10/15	183	5.35	53.5	0.69
	Pessimistic	509	3.4	05/01–09/30	153	4.78	47.8	0.74
Alternative reactor design: 7 year usage of PMMA with reduced PCE	Optimistic	628	3.3	04/01–10/31	214	5.75	57.5	0.51
	Intermediate	628	3.3	04/15–10/15	183	5.19	51.9	0.54
	Pessimistic	628	3.3	05/01–09/30	153	4.64	46.4	0.58

0.010 $\text{kg PO}_4^- \text{eq kg}^{-1} \text{ DM}$ and is mainly caused by spoil from lignite mining for the production of electricity. The acidification potential has a distribution of values comparable with the global warming potential and is mostly due to the use of ammonium fertilizer, cleaning with hydrogen peroxide, and the emittance of sulfur dioxide arising from biogas, which is used for electricity. Acidification is especially high in the PMMA scenarios and lies between 0.014 and 0.017 $\text{kg SO}_2 \text{eq kg}^{-1} \text{ DM}$ for the 3-year PMMA scenarios and 0.009 and 0.014 $\text{kg SO}_2 \text{eq kg}^{-1} \text{ DM}$ for the 7-year PMMA scenarios. Again, the extended use of acrylic glass tubes drastically reduces the acidification potential even though productivity is diminished in these scenarios. The exact CML IA baseline values for all scenarios are shown in Table 2.

The cumulative energy demand (Fig. 4) is clearly dominated by the sum of electricity processes, especially electricity for mixing (8.7–11.1 $\text{MJ kg}^{-1} \text{ DM}$), centrifugation (9.0 $\text{MJ kg}^{-1} \text{ DM}$), and drying (10.4 $\text{MJ kg}^{-1} \text{ DM}$). This result is due to the energy originating largely from fossil and nuclear energy sources. Another critical process is hydrogen peroxide, which causes values between 11.9 and 18.8 $\text{MJ kg}^{-1} \text{ DM}$. Concerning the scenarios with acrylic glass, the infrastructure represents the greatest share of energy use in these scenarios, which is caused by the energy-intensive production of PMMA. Thus, the 3-year use of the PMMA tubes produces 37.2 and 46.1 $\text{MJ kg}^{-1} \text{ DM}$, whereas energy use can be reduced to 15.5 and 19.2 $\text{MJ kg}^{-1} \text{ DM}$ in the 7-year use of the PMMA tubes. However, all scenarios highly benefit from the avoidance of CO_2 , which results in a reduction of 17.6 $\text{MJ kg}^{-1} \text{ DM}$ for every scenario due to the use of fossil energy sources. A detailed overview of the CED values of all subprocesses is included in the supplementary material (Table S5). The total CED values for each scenario are included in Table 2.

Water scarcity is assessed through the water stress index (WSI) according to Hoekstra et al. (2012), the total blue water use according to the LCI values, and the potential water deprivation according to AWARE. Following the water stress index (Fig. 5), the microalgae cultivation scenarios use between 0.04 and 0.06 $\text{m}^3 \text{ kg}^{-1} \text{ DM}$. The water use values from the LCI illustrate the consumptions of the particular cultivation stages and are portrayed by bars in Fig. 4. Most of the water is consumed due to hydrogen peroxide use and freshwater consumption for cleaning, the initial filling, and filling after harvest. Concerning the acrylic glass scenarios, PMMA is again a critical process. The potential for water deprivation (Fig. 6) portrays values between 1.7 and 2.8 $\text{m}^3 \text{ kg}^{-1} \text{ DM}$ which are caused by the same sources as the values in the water stress index. In all water assessment methods, it can be observed that it is favorable to have an extended cultivation season. The optimistic scenarios always exhibited the lowest damage in each scenario set. The exact values are shown in the supplementary material for water use (Table S3) and in Table 2 for water scarcity.

Table 2 Environmental impacts per kg of dry microalgae biomass, according to cultivation scenarios

	Na.sp. Glass 40 mm pes.	Na.sp. Glass 40 mm int.	Na.sp. Glass 40 mm opt.	Na.sp. Glass 36 mm pes.	Na.sp. Glass 36 mm int.	Na.sp. Glass 36 mm opt.	Na.sp. PMMA 3 years pes.	Na.sp. PMMA 3 years int.
Global warming in kg CO ₂ eq kg ⁻¹	1.69	1.62	1.58	1.42	1.38	1.35	4.70	4.32
Acidification in kg SO ₂ eq kg ⁻¹	0.00440	0.00422	0.00407	0.00358	0.00347	0.00338	0.01651	0.01504
Eutrophication in kg PO ₄ eq kg ⁻¹	0.00874	0.00866	0.00860	0.00810	0.00804	0.00802	0.00977	0.00957
WSI in m ³ kg ⁻¹	0.052	0.047	0.043	0.043	0.039	0.036	0.059	0.054
AWARE in m ³ kg ⁻¹	2.433	2.202	2.016	2.005	1.818	1.667	2.830	2.556
Land use in m ² kg ⁻¹	0.209	0.187	0.169	0.209	0.187	0.169	0.209	0.187
CED in MJ kg ⁻¹	37.22	35.58	34.29	32.31	31.05	30.06	82.16	75.73

	Na.sp. PMMA 3 years opt.	Na.sp. PMMA 7 years pes.	Na.sp. PMMA 7 years int.	Na.sp. PMMA 7 years opt.	Ph.tr. Glass 40 mm pes.	Ph.tr. Glass 40 mm int.	Ph.tr. Glass 40 mm opt.
Global warming in kg CO ₂ eq kg ⁻¹	4.02	2.96	2.77	2.61	1.76	1.70	1.65
Acidification in kg SO ₂ eq kg ⁻¹	0.01385	0.00953	0.00881	0.00822	0.00478	0.00459	0.00445
Eutrophication in kg PO ₄ eq kg ⁻¹	0.00943	0.00902	0.00892	0.00885	0.00881	0.00872	0.00867
WSI in m ³ kg ⁻¹	0.050	0.056	0.051	0.047	0.051	0.047	0.043
AWARE in m ³ kg ⁻¹	2.336	2.661	2.408	2.200	2.421	2.192	2.009
Land use in m ² kg ⁻¹	0.169	0.216	0.193	0.174	0.204	0.182	0.165
CED in MJ kg ⁻¹	70.58	56.12	52.53	49.63	37.38	35.71	34.44

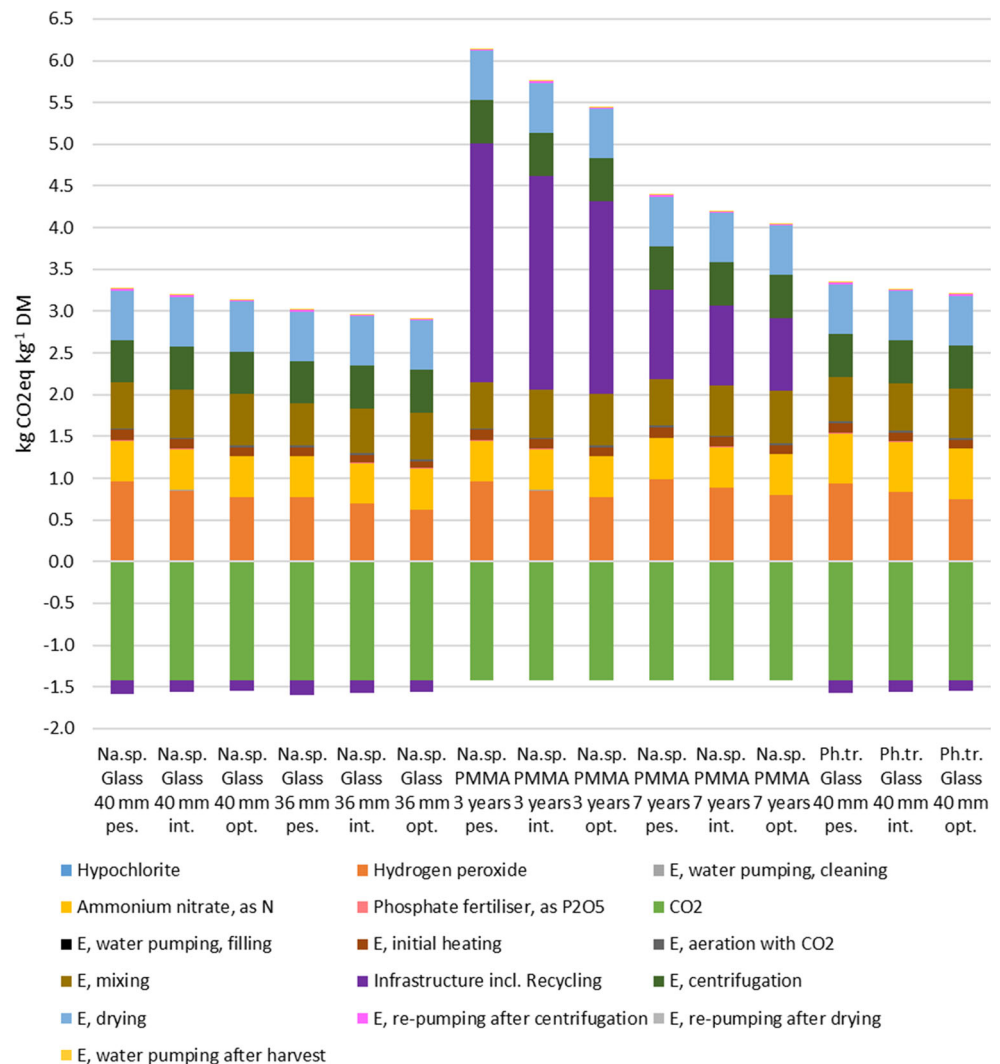
Sensitivity analysis

Sensitivity analysis was performed in terms of a series of scenarios that evaluated fluctuations in climatic preconditions and different technological design choices, which might be a more optimized option. Microalgae cultivation strongly depends on solar insolation and temperature. Consequently, three different scenarios with varied lengths of the cultivation season were considered. The detailed evaluation of the climatic data revealed that temperatures can occasionally drop below 0 °C in April and October. In the optimistic scenario, it was assumed that temperatures do not fall below 0 °C in April and October, and cultivation would be feasible throughout these months. The intermediate scenario assumed production from mid-April until mid-October. The pessimistic scenario expected April and October to be too cold for cultivation and comprised cultivation from May until September. The long (optimistic) production period involved reduced productivity. The analysis of the results revealed that a long production period was always favorable over short cultivation seasons. The optimistic scenarios portrayed the lowest environmental impacts for each microalgae scenario set.

As a second variation, the tube diameter was altered from 40 to 36 mm to investigate the corresponding shifts in the impact results. The thin tubes dictated a reduced PBR volume, while the productivity was expected to remain constant assuming that the biomass concentration in the suspension would increase. Again, the optimistic, intermediate, and pessimistic scenarios were analyzed for the decreased diameter. Consequently, the energy use per kg DM increased for freshwater pumping at the cleaning and cultivation stage and for the initial heating of the PBR. However, all other processes showed reduced environmental burdens. Thus, the 36-mm scenarios overall mostly portrayed the least environmental impacts.

Furthermore, PMMA as a material for the tubes and PP for the corners were tested because they were classified in the literature as appropriate PBR materials and have already been applied in pilot-scale facilities. Since PMMA quickly degrades under UV radiation, production scenarios over 3 and 7 years with subsequent recycling of the tubes were evaluated with each option being tested in the optimistic, intermediate, and pessimistic scenarios. The 7-year usage of PMMA comprised a reduced PCE to account for the degradation of the material. Although the PMMA scenarios were mostly the least favorable among the microalgae scenarios in terms of environmental impacts, the difference in environmental impacts was not tremendous. Thus, it is worthwhile to compare the environmental impacts from the PMMA scenarios to those from other food groups on a nutritional basis. Microalgae cultivation in PMMA tubes should not per se be excluded as a compatible option.

Fig. 2 Global warming potential of microalgae cultivation in $\text{CO}_2\text{eq kg}^{-1}$ DM, according to IPCC 2013 GWP 100, (E, Electricity)



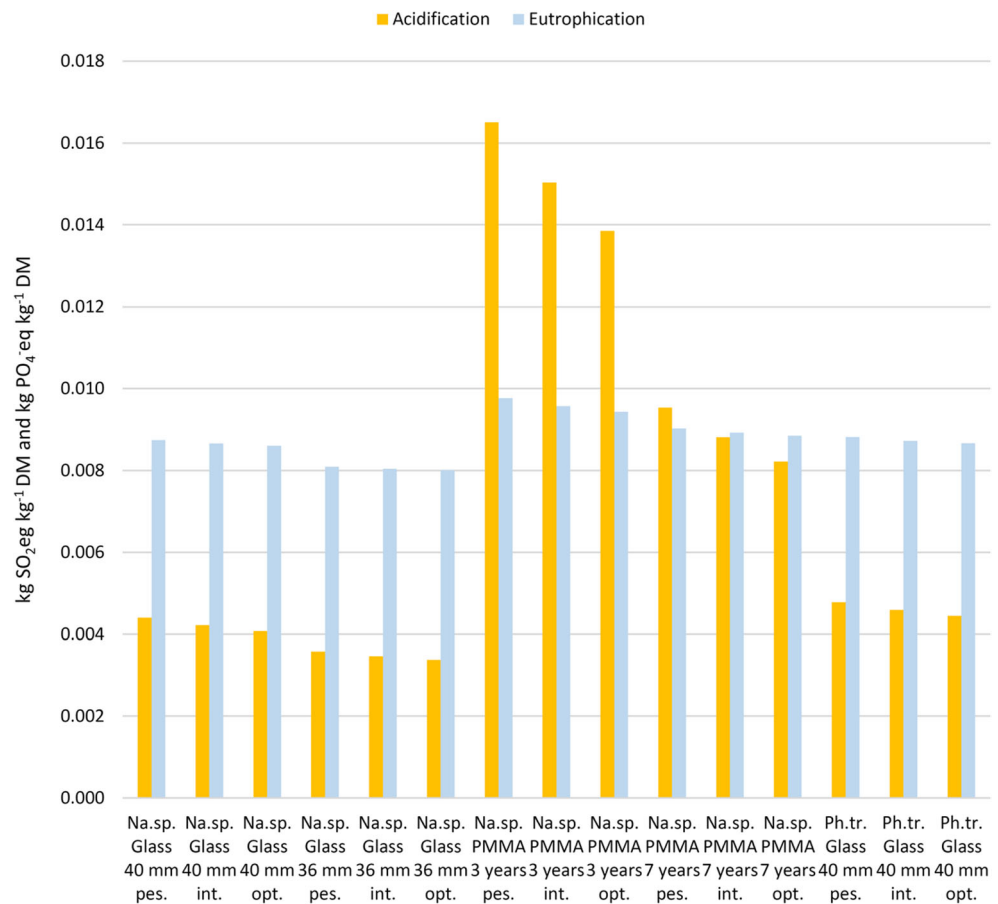
Moreover, the cultivation of another microalgae species, namely, *P. tricorutum*, was assessed in 40 mm borosilicate tubes to evaluate the variations arising from a microalga with slightly different nutritional values. The choice of a microalgae species with slightly different nutritional values had only a marginal impact on the overall results, which were comparable with those from the cultivation of *Nannochloropsis* sp. in 40-mm borosilicate glass tubes. The *P. tricorutum* scenarios, however, were found to have slightly higher yields but also marginally higher environmental impacts than the *Nannochloropsis* sp. scenarios.

Uncertainty analysis

Monte Carlo simulation was applied for the analysis of uncertainty. As background processes were taken from Ecoinvent v.3.4, these data were already supplied with a distribution factor. Concerning data from our own calculations, uncertainty was assessed using the Pedigree matrix and a lognormal

distribution. The uncertainty for all electrical processes was calculated as 1.07 using the Pedigree matrix. The uncertainty for all other processes (PBR materials, nutrients, land and water use) was calculated as 1.13 from the Pedigree matrix. Screenshots of the filled Pedigree matrices can be accessed in the supplementary material (Figs. S3–S4). The baseline scenario (*Nannochloropsis* sp., 40-mm borosilicate glass tubes, intermediate cultivation season) was tested against all other scenarios (diameter variations, optimistic and pessimistic cultivation seasons, 7-year PMMA lifespan, and microalgae species variations). Additionally, the PMMA scenario with a 3-year lifespan of tubes was tested against the scenario with the 7-year lifespan. Monte Carlo simulations were always run 1000 times for each scenario comparison using IPCC 2013 GWP 100a. The exact results of the Monte Carlo simulations are shown in Table 3, including the 95% confidence interval, median, and outcome for every scenario combination. The uncertainty analysis confirmed the differences between the microalgae scenarios to be significant with a confidence

Fig. 3 Acidification potential in kg SO₂eq kg⁻¹ DM and eutrophication potential in kg PO₄⁻eq kg⁻¹ DM, according to CML IA Baseline EU25



interval of at least 95%. Figures on the Monte Carlo analysis can be accessed in the supplementary material (Figs. S5–S10).

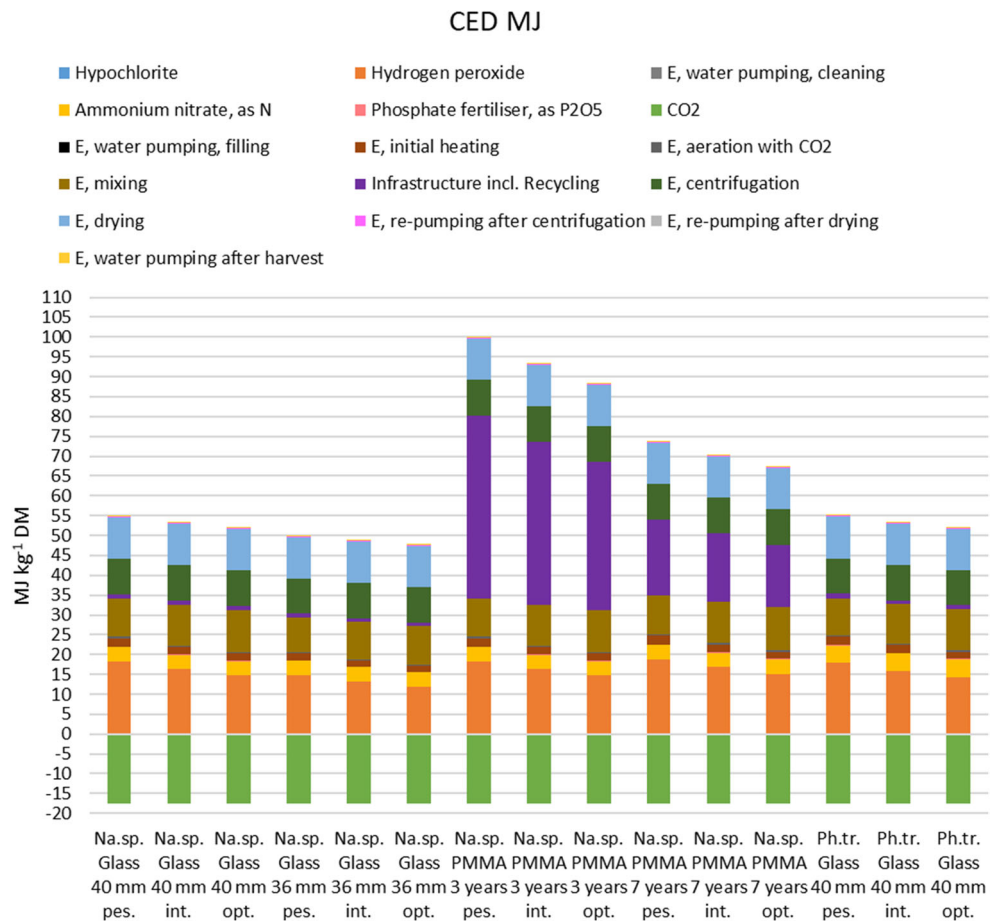
Discussion

Our analysis assessed the environmental impacts of industrial-scale microalgae cultivation in Germany using a computable “top-down” approach to investigate the relevant input flows. It was shown that the developed methodology could possibly be applied to different microalgae cultivation scenarios, including different locations worldwide, using satellite climatic data. Parameter variations were tested concerning the tube diameter, the tube material, an alternative microalgae species, and different cultivation season lengths. Borosilicate glass as the tube material was found to be favorable, although PMMA did not perform tremendously worse and could be a decent option for the reactor tubes. A small tube diameter was clearly favorable and had the least environmental impacts in all scenarios. Moreover, it was determined that an extended cultivation season from April until October is preferable, if possible. Even though productivity was reduced in spring and fall (solar insolation in April on average is decreased by 3.9 MJ m⁻² day⁻¹ compared with that in May, whereas it drops by 5.2 MJ m⁻² day⁻¹ on average from

September to October), a longer cultivation season still had smaller environmental impacts than a shorter season with increased productivity. More specifically, the global warming potential was reduced by 0.11 kg CO₂eq kg⁻¹ DM when cultivation took place every year from April 1 until October 31 instead of from May 1 until September 30. For the same cultivation season shift, acidification decreased by 0.33 g kg⁻¹ DM, eutrophication decreased by 0.14 g kg⁻¹ DM, and the CED decreased by 2.93 MJ kg⁻¹ DM. Land and water use (WSI) declined by 0.04 m² kg⁻¹ DM and 9 L kg⁻¹ DM, respectively. An even longer cultivation season before April and after October was not investigated, as it would not have been consistent with the methodological approach in this study, which excluded months where the temperature was lower than 0 °C.

Critical processes in all scenarios above all were the usage of hydrogen peroxide for the sterilization of the PBR tubes at the cleaning stage. Moreover, nitrogen fertilizer had relatively high environmental impacts. Another bottleneck was electricity use, in particular for mixing of the suspension in the tubes during cultivation and for centrifugation and drying at the harvest stage. The high impacts of the electricity processes were mainly due to the application of a regular electricity mix that was primarily composed of nonrenewable energy sources, such as hard coal and lignite.

Fig. 4 Cumulative energy demand in MJ kg⁻¹ DM, (E, Electricity)



The comparison to the results of preceding environmental assessments of microalgae cultivation is difficult due to differing system boundaries, functional units, target products, and cultivation systems. Additionally, numerous types of LCIA methods exist, which distort comparisons to some extent. The greatest restraint for comparison is probably finding analyses with similar system boundaries and scales. As described in “Materials and methods” section, many preceding studies focused on the production of microalgae for some kind of biofuel. Thus, the results were often shown for the whole production process, including downstream processing, rather than giving results for particular stages of production. As in

this study, the cultivation stage up to dry biomass was investigated; thus, a comparison to biofuel assessments is inappropriate.

Concerning productivity, Silva et al. (2015) reported a dry biomass production rate of 1.5 kg m⁻³ day⁻¹ (1.5 g L⁻¹ day⁻¹) for a tubular PBR located in Brazil. This rate is almost three times the productivity determined in this study (baseline, 0.56 g L⁻¹ day⁻¹), which could partly be attributed to more favorable climatic conditions in Brazil. Taelman et al. (2013) assessed microalgae biomass production on a 2.5 ha scale in Spain (extrapolated from the pilot scale) where *Nannochloropsis* sp. was cultivated in ProviAPT

Fig. 5 Water stress index according to Hoekstra et al. (2012) and blue water use in m³ kg⁻¹ DM

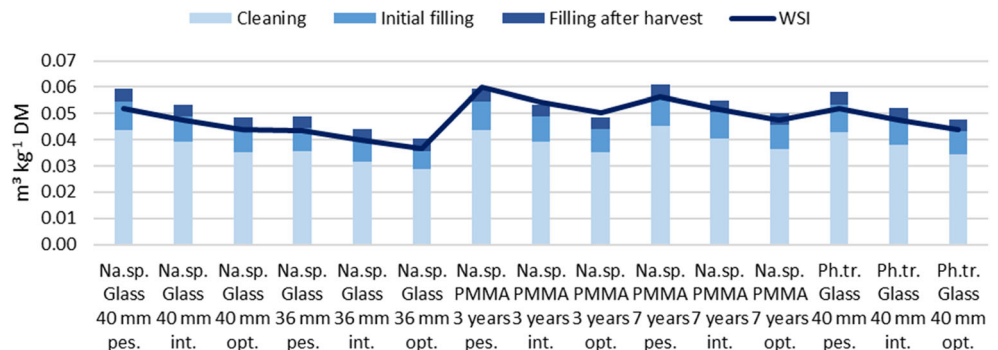
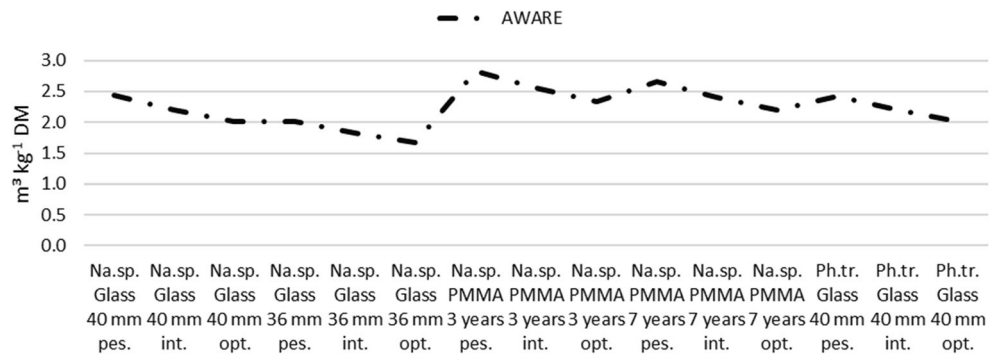


Fig. 6 Potential water deprivation in $\text{m}^3 \text{kg}^{-1} \text{DM}$, according to AWARE



photobioreactors (plastic bags). This system generated a carbon footprint of $0.09 \text{ kg CO}_2\text{eq MJ}^{-1}$ of exergy DM ($\sim 1.6 \text{ kg CO}_2\text{eq kg}^{-1} \text{ DM}$), which is similar to the baseline scenario in this study. Collotta et al. (2018) investigated the production of *Chlorella vulgaris* dry biomass in Canada in an ORP with similar system boundaries as this study. A climate change potential of $1.641 \text{ kg CO}_2\text{eq kg}^{-1} \text{ DM}$ was reported. Armstrong assessed the cultivation of *Nannochloropsis salina* in a PBR in Colorado, USA, with comparable system boundaries (Armstrong 2013). The growth rate of $57,165 \text{ kg ha}^{-1} \text{ year}^{-1}$ ($57.2 \text{ t ha}^{-1} \text{ year}^{-1}$) is similar to the baseline scenario in this study ($53.5 \text{ t ha}^{-1} \text{ year}^{-1}$). The total energy consumption during cultivation was $7.42 \text{ MJ kg}^{-1} \text{ DM}$, while the baseline scenario of this study had increased energy consumption of $10.6 \text{ MJ kg}^{-1} \text{ DM}$.

To use the model under other conditions, various changes are easily feasible due to the transparent construction of the system. Thus, it is possible to vary the facility location, seasons, scale,

tube dimensions and material, microalgae species, nutrient inputs, and flow velocity. Moreover, single processes can easily be complemented or exchanged to further adjust the model individually, if, for instance, another downstream pathway is required. For the extraction of single nutrients, for example, individual calculations for downstream processing could be added, either starting from the dry biomass or omitting the drying stage for wet extraction. Upon the variations in these parameters, further aspects that will shift because of the variation need to be considered. Hence, the cultivation of another microalgae species could possibly require other cultivation conditions, such as another optimum temperature and different nutrient requirements. The constant adaptation of the suspension temperature through mixing of evaporated and freshly pumped water should make further heating or cooling redundant. However, in a previous study by the authors, it was observed that cultivation in PBRs might be most suitable in locations where solar insolation does not exceed $21 \text{ MJ m}^{-2} \text{ day}^{-1}$ (Schade and Meier 2019). A drastic

Table 3 The 95% confidence interval, median and outcome for Monte Carlo simulations of scenario comparisons

Scenario calculation	2.5%	97.5%	Median	Outcome
Na.sp., glass, 36 mm, int. (A) minus Na.sp., glass, 40 mm, int. (B)	-0.294	-0.203	-0.244	GWP (A) < GWP (B)
Na.sp., glass, 40 mm, opt. (A) minus Na.sp., glass, 40 mm, int. (B)	-0.075	-0.026	-0.046	GWP (A) < GWP (B)
Na.sp., glass, 40 mm, pes. (A) minus Na.sp., glass, 40 mm, int. (B)	0.035	0.095	0.061	GWP (A) > GWP (B)
Na.sp., glass, 40 mm, int. (B) minus Na.sp., glass, 40 mm, int. (A)	-1.294	-0.975	-1.142	GWP (A) < GWP (B)
Na.sp., PMMA, 7 years, int. (B) minus Na.sp., PMMA, 3 years, int. (A)	1.371	1.758	1.553	GWP (A) > GWP (B)
Na.sp., PMMA, 7 years, int. (B) minus Na.sp., glass, 40 mm, int. (A)	-0.128	-0.036	-0.071	GWP (A) < GWP (B)
Ph.tr., glass, 40 mm, int. (B)				

variation in the tube diameter should entail a reconsideration of the PCE, which should be corrected downwards with a remarkably increased diameter. The flow velocity should be set in accordance with the microalgae species to avoid settling caused by too little velocity or cell destruction provoked by a rather high flow velocity.

Some aspects could not be covered in this study but should be investigated in future studies. One scenario used a slightly reduced tube diameter and relied on the assumptions that the areal productivity remains constant. It could be evaluated at the laboratory and pilot scales how exactly microalgae cultivation productivity responds to alterations in tube diameter. In this context, the evaluation of further suitable microalgae species is advisable, as the usage of alternative microalgae species can significantly alter the results. The results also suggested that PMMA could be a feasible material for the reactor tubes, as the 7-year scenario performed drastically better than the 3-year PMMA scenario. A comprehensive investigation of acrylic glass for reactors should be conducted, above all concerning the safety concerning the production of edibles. This study further relied on the usage of an average electricity mix for Germany regarding the energy processes for microalgae cultivation. As this electricity mix mainly comprised nonrenewable energies, it would be very relevant to repeat the assessment with an increased share of renewable energy sources.

At some points of the study, foreground data were derived from the literature, which we indicated in the methodological section (“**Materials and methods**” section.). However, if possible, average data were adopted from different studies with similar conditions concerning the particular parameter. Additionally, only values that were consistent with the system settings were used in this study.

The methodological approach conducted in this study can be applied in further analyses on tubular PBRs, while the parameters can be adjusted to a multiplicity of different scenarios. Furthermore, the detailed microalgae data obtained from this study can be used in other environmental assessments to compare the impacts of microalgae or products made of microalgae to other products and product categories. The exact LCI and LCIA values were included per kg DM in the supplementary material, which should provide a good basis for further studies. Moreover, the LCIA categories used are relevant on a global scale.

Conclusion

Our computational model can be utilized to assess the complete input flows to microalgae cultivation in a tubular PBR. Parameter variation is possible to a great extent which allows application of the model to numerous different locations and settings. The testing of the model in a location in Germany, as an example of a “cold-weather” climate,

showed that microalgae cultivation in such a climate can be sustainable. Even though productivity is decreased in spring and fall due to reduced solar insolation and temperatures, it is nevertheless preferable to have a long cultivation season comprising April and October instead of having a short cultivation season with a high average productivity. Moreover, a reduced tube diameter could be favorable to reduce the cultivation costs. The most critical processes comprised the use of hydrogen peroxide for cleaning and energy processes at the harvest stage.

Acknowledgements Open Access funding provided by Projekt DEAL.

Funding information The study was funded by the Federal Ministry of Education and Research (FKZ: 031B0366A).

Compliance with ethical standards

Conflict of interest The authors declare that they have no conflict of interests.

Open Access This article is licensed under a Creative Commons Attribution 4.0 International License, which permits use, sharing, adaptation, distribution and reproduction in any medium or format, as long as you give appropriate credit to the original author(s) and the source, provide a link to the Creative Commons licence, and indicate if changes were made. The images or other third party material in this article are included in the article's Creative Commons licence, unless indicated otherwise in a credit line to the material. If material is not included in the article's Creative Commons licence and your intended use is not permitted by statutory regulation or exceeds the permitted use, you will need to obtain permission directly from the copyright holder. To view a copy of this licence, visit <http://creativecommons.org/licenses/by/4.0/>.

References

- Acién Fernández FG, Fernández Sevilla JM, Sánchez Pérez JA, Molina Grima E, Chisti Y (2001) Airlift-driven external-loop tubular photobioreactors for outdoor production of microalgae: assessment of design and performance. *Chem Eng Sci* 56:2721–2732
- Al Hattab M, Ghaly A, Hammouda A (2015) Microalgae harvesting methods for industrial production of biodiesel: critical review and comparative analysis. *J Fundam Renew Energy* 5. <https://doi.org/10.4172/20904541.1000154>
- Armstrong KO (2013) Analysis of life cycle assessment of food/energy/waste systems and development and analysis of microalgae cultivation/wastewater treatment inclusive system. Colorado State University, USA, MSc Thesis
- Barros AI, Gonçalves AL, Simões M, Pires JCM (2015) Harvesting techniques applied to microalgae: a review. *Renew Sust Energy Rev* 41: 1489–1500
- Bartley ML, Boeing WJ, Dungan BN, Omar Holguin F, Schaub T (2014) pH effects on growth and lipid accumulation of the biofuel microalgae *Nannochloropsis salina* and invading organisms. *J Appl Phycol* 26:1431–1437
- Batan L, Quinn J, Willson B, Bradley T (2010) Net energy and greenhouse gas emission evaluation of biodiesel derived from microalgae. *Environ Sci Technol* 44:7975–7980

- Benemann J (2013) Microalgae for biofuels and animal feeds. *Energies* 6: 5869–5886
- Bennion EP, Ginosar DM, Moses J, Agblevor F, Quinn JC (2015) Lifecycle assessment of microalgae to biofuel: comparison of thermochemical processing pathways. *Appl Energy* 154:1062–1071
- Borowitzka M (2018) Commercial-scale production of microalgae for bioproducts. In: La Barre S, Bates S (eds) *Blue biotechnology: production and use of marine molecules*, vol 1. Wiley-VCH, Weinheim, pp 33–65
- Borowitzka M (2013) *Dunaliella*: biology, production, and markets. In: Richmond A, Hu Q (eds) *Handbook of microalgal culture: applied phycology and biotechnology*. John Wiley & Sons, Ltd, Chichester, UK, pp 359–368
- Boulay AM, Bare J, Benini L, Berger M, Lathuilière MJ, Manzardo A, Margni M, Motoshita M, Núñez M, Pastor AV, Ridoutt B, Oki T, Worbe S, Pfister S (2018) The WULCA consensus characterization model for water scarcity footprints: assessing impacts of water consumption based on available water remaining (AWARE). *Int J Life Cycle Assess* 23:368–378
- Burgess G, Fernández-Velasco JG (2007) Materials, operational energy inputs, and net energy ratio for photobiological hydrogen production. *Int J Hydrog Energy* 32:1225–1234
- Campbell PK, Beer T, Batten D (2011) Life cycle assessment of biodiesel production from microalgae in ponds. *Bioresour Technol* 102:50–56
- Caporgno MP, Mathys A (2018) Trends in microalgae incorporation into innovative food products with potential health benefits. *Front Nutr* 5:1–10
- Cazcarro I, López-Morales CA, Duchin F (2019) The global economic costs of substituting dietary protein from fish with meat, grains and legumes, and dairy. *J Ind Ecol* 2:1–13
- Chini Zittelli G, Lavista F, Bastianini A, Rodolfi L, Vincenzini M, Tredici MR (1999) Production of eicosapentaenoic acid by *Nannochloropsis* sp. cultures in outdoor tubular photobioreactors. *J Biotechnol* 70:299–312
- Chisti Y (2007) Biodiesel from microalgae. *Biotechnol Adv* 25:294–306
- Collet P, Hélias A, Lardon L, Ras M, Goy RA, Steyer JP (2011) Life-cycle assessment of microalgae culture coupled to biogas production. *Bioresour Technol* 102:207–214
- Collet P, Lardon L, Hélias A, Bricout S, Lombaert-Valot I, Perrier B, Lépine O, Steyer JP, Bernard O (2014) Biodiesel from microalgae - life cycle assessment and recommendations for potential improvements. *Renew Energy* 71:525–533
- Collotta M, Champagne P, Mabee W, Tomasoni G (2018) Wastewater and waste CO₂ for sustainable biofuels from microalgae. *Algal Res* 29:12–21
- de Bruijn H, van Duin R, Huijbregts MAJ (2002) *Handbook on life cycle assessment*. Springer Netherlands, Dordrecht
- de Vree JH, Bosma R, Janssen M, Barbosa MJ, Wijffels RH (2015) Comparison of four outdoor pilot-scale photobioreactors. *Biotechnology for Biofuels* 8(1)
- Engineering ToolBox (2003a) Pump Power Calculator
- Engineering ToolBox (2005) Carbon Dioxide Gas - Specific Heat. https://www.engineeringtoolbox.com/carbon-dioxide-d_974.html
- Engineering ToolBox (2003b) Water - Thermophysical Properties. https://www.engineeringtoolbox.com/water-thermal-properties-d_162.html
- Enzing C, Ploeg M, Barbosa M, Sijtsma L (2014) Micro-algal production systems
- Fábregas J, Maseda A, Domínguez A, Otero A (2004) The cell composition of *Nannochloropsis* sp. changes under different irradiances in semicontinuous culture. *World J Microbiol Biotechnol* 20:31–35
- Fasaei F, Bitter JH, Slegers PM, van Boxtel AJB (2018) Techno-economic evaluation of microalgae harvesting and dewatering systems. *Algal Res* 31:347–362
- Frischknecht R, Jungbluth N, Althaus H, Bauer C, Doka G, Dones R, Hischier R, Hellweg S, Humbert, Köllner T, Loerincik Y, Margni M, Nemecek T (2007) Implementation of life cycle impact assessment methods. ecoinvent report No. 3, v2.0. Swiss Centre for Life Cycle Inventories. 151 p
- Greenwell HC, Laurens LML, Shields RJ, Lovitt RW, Flynn KJ (2010) Placing microalgae on the biofuels priority list: a review of the technological challenges. *J R Soc Interface* 7:703–726
- Grierson S, Strezov V, Bengtsson J (2013) Life cycle assessment of a microalgae biomass cultivation, bio-oil extraction and pyrolysis processing regime. *Algal Res* 2:299–311
- Gu N, Lin Q, Li G, Tan Y, Huang L, Lin J (2012) Effect of salinity on growth, biochemical composition, and lipid productivity of *Nannochloropsis oculata* CS 179. *Eng Life Sci* 12:631–637
- Gutiérrez-Salmeán G, Fabila-Castillo L, Chamorro-Cevallos G (2015) Nutritional and toxicological aspects of *Spirulina (Arthrospira)*. *Nutr Hosp* 32:34–40
- Hoekstra AY, Mekonnen MM, Chapagain AK, Mathews RE, Richter BD (2012) Global monthly water scarcity: blue water footprints versus blue water availability. *PLoS One* 7:0032688
- Hou J, Zhang P, Yuan X, Zheng Y (2011) Life cycle assessment of biodiesel from soybean, jatropha and microalgae in China conditions. *Renew Sust Energ Rev* 15:5081–5091
- Huang Q, Jiang F, Wang L, Yang C (2017) Design of photobioreactors for mass cultivation of photosynthetic organisms. *Engineering*. 3: 318–329
- Hulatt CJ, Wijffels RH, Bolla S, Kiron V (2017) Production of fatty acids and protein by *Nannochloropsis* in flat-plate photobioreactors. *PLoS One* 12:e0170440
- IPCC (2014) *Climate change 2014: synthesis report*. Contribution of working groups I, II and III to the Fifth Assessment Report of the Intergovernmental Panel on Climate Change. IPCC, Geneva, Switzerland
- ISO Organisation (2006) *ISO 14044:2006 - Environmental Management - Life Cycle Assessment - Requirements and Guidelines*. Genf
- Kaminsky W, Eger C (2001) Pyrolysis of filled PMMA for monomer recovery. *J Anal Appl Pyrolysis* 58–59:781–787
- Keller H, Reinhardt GA, Rettenmaier N, Schorb A, Dittrich M (2017) Environmental assessment of algae-based PUFA production. IFEU, Heidelberg
- Kent M, Welladsen HM, Mangott A, Li Y (2015) Nutritional evaluation of Australian microalgae as potential human health supplements. *PLoS One* 10:e0118985
- Khatoun H, Abdu Rahman N, Banerjee S, Harun N, Suleiman SS, Zakari NH, Lananan N, Hamid SHA, Endut A (2014) Effects of different salinities and pH on the growth and proximate composition of *Nannochloropsis* sp. and *Tetraselmis* sp. isolated from South China Sea cultured under control and natural condition. *Int Biodeterior Biodegrad* 95:11–18
- Khoo HH, Sharratt PN, Das P, Balasubramanian RK, Narahariseti PK, Shaik S (2011) Life cycle energy and CO₂ analysis of microalgae-to-biodiesel: preliminary results and comparisons. *Bioresour Technol* 102:5800–5807
- Lardon L, Helias A, Sialve B et al (2009) Life-cycle assessment of biodiesel production from microalgae. *Environ Sci Technol* 43:6475–6481
- Lundquist T, Woertz I, Quinn N, Benemann J (2010) A realistic technology and engineering assessment of algae biofuel production. Energy Biosciences Institute, Berkeley
- Ma XN, Chen TP, Yang B, Liu J, Chen F (2016) Lipid production from *Nannochloropsis*. *Mar Drugs* 14:61
- Mišurová L, Škrovánková S, Samek D, Ambrožová J, Machů L (2012) Health benefits of algal polysaccharides in human nutrition. *Adv Food Nutr Res* 66:75–145
- Molino A, Iovine A, Casella P, Mehariya S, Chianese S, Cerbone A, Rimauro J, Musmarra D (2018) Microalgae characterization for consolidated and new application in human food, animal feed and nutraceuticals. *Int J Environ Res Public Health* 15:2436

- Monari C, Righi S, Olsen SI (2016) Greenhouse gas emissions and energy balance of biodiesel production from microalgae cultivated in photobioreactors in Denmark: a life-cycle modeling. *J Clean Prod* 112:4084–4092
- NASA - National Aeronautics, Space Administration (2019) Power Data Access Viewer. <https://power.larc.nasa.gov/data-access-viewer/>
- Norsker N-H, Barbosa M, Vermue M, Wijffels R (2012) On energy balance and production costs in tubular and flat panel photobioreactors. *Technik* 21:54–62
- Olofsson M, Lindehoff E, Frick B, Svensson F, Legrand C (2015) Baltic Sea microalgae transform cement flue gas into valuable biomass. *Algal Res* 11:227–233
- Paes CRPS, Faria GR, Tinoco NAB, Castro DFJA, Barbarino E, Lourenco SO (2016) Growth, nutrient uptake and chemical composition of *Chlorella* sp. and *Nannochloropsis oculata* under nitrogen starvation. *Lat Am J Aquat Res* 44:275–292
- Pahl SL, Lee AK, Kalaitzidis T, Ashman PJ, Sathe S, Lewis DM (2013) Harvesting, thickening and dewatering microalgae biomass. In: Borowitzka MA, Moheimani NR (eds) *Algae for biofuels and energy*. Springer, Dordrecht, pp 165–185
- Parodi A, Leip A, De Boer IJM, Slegers PM, Ziegler F, Temme EHM, Herrero M, Tuomisto H, Valin H, VanMiddelaa CE, VanLoon JJA, VanZanten HHE (2018) The potential of future foods for sustainable and healthy diets. *Nat Sustain* 1:782–789
- Patil V, Tran KQ, Giselrød HR (2008) Towards sustainable production of biofuels from microalgae. *Int J Mol Sci* 9:1188–1195
- Pérez-López P, de Vree JH, Feijoo G, Bosma R, Barbosa MJ, Moreira MT, Wijffels RH, van Boxtel AJB, Kleinegris DMM (2017) Comparative life cycle assessment of real pilot reactors for microalgae cultivation in different seasons. *Appl Energy* 205:1151–1164
- Pérez-López P, González-García S, Jeffryes C, Agathos SN, McHugh E, Walsh D, Murray P, Moane S, Feijo G, Moreira MT (2014) Life cycle assessment of the production of the red antioxidant carotenoid astaxanthin by microalgae: from lab to pilot scale. *J Clean Prod* 64:332–344
- Perugini F, Mastellone ML, Arena U (2005) A life cycle assessment of mechanical and feedstock recycling options for management of plastic packaging wastes. *Environ Prog* 24:137–154
- Petkov GD, Bratkova SG (1996) Viscosity of algal cultures and estimation of turbulence in devices for the mass culture of microalgae. *Arch Hydrobiol* 81:99–104
- Pipe Flow Software (2019) Pipe Roughness. <https://www.pipeflow.com/pipe-pressure-drop-calculations/pipe-roughness>
- Posten C (2012) Design and performance parameters of photobioreactors. *Tech - Theor Prax* 21:38–45
- Quinn JC, Smith TG, Downes CM, Quinn C (2014) Microalgae to biofuels lifecycle assessment - multiple pathway evaluation. *Algal Res* 4:116–122
- Raghuvanshi S, Bhakar V, Chava R, Sangwan KS (2018) Comparative study using life cycle approach for the biodiesel production from microalgae grown in wastewater and fresh water. *Procedia CIRP* 69:568–572
- Rasdi NW, Qin JG (2015) Effect of N:P ratio on growth and chemical composition of *Nannochloropsis oculata* and *Tisochrysis lutea*. *J Appl Phycol* 27:2221–2230
- Reboloso-Fuentes M, Navarro-Perez A, Ramos-Miras JJ, Guil-Guerrero JL (2007) Biomass nutrient profiles of the microalga *Phaeodactylum tricornutum*. *J Food Biochem* 25:57–76
- Reboloso-Fuentes MM, Navarro-Pérez A, García-Camacho F, Ramos-Miras JJ, Guil-Guerrero JL (2001) Biomass nutrient profiles of the microalga *Nannochloropsis*. *J Agric Food Chem* 49:2966–2972
- Rocha JMS, Garcia JEC, Henriques MHF (2003) Growth aspects of the marine microalga *Nannochloropsis gaditana*. *Biomol Eng* 20:237–242
- Ryckebosch E, Bruneel C, Termote-Verhalle R, Goiris K, Muylaert K, Foubert I (2014) Nutritional evaluation of microalgae oils rich in omega-3 long chain polyunsaturated fatty acids as an alternative for fish oil. *Food Chem* 160:393–400
- Safar H, Hass MZ, Møller P, Holdt SL, Jacobsen C (2016) High-EPA biomass from *Nannochloropsis salina* cultivated in a flat-panel photo-bioreactor on a process water-enriched growth medium. *Mar Drugs* 14:144
- Safi C, Zebib B, Merah O, Pontalier P-Y (2014) Morphology, composition, production, processing and applications of *Chlorella vulgaris*: a review. *Renew Sust Energ Rev* 35:265–278
- Schade S, Meier T (2019) A comparative analysis of the environmental impacts of cultivating microalgae in different production systems and climatic zones: a systematic review and meta-analysis. *Algal Res* 40:101485
- Schade S, Stangl GI, Meier T (2020) Distinct microalgae species for food – part 2: comparative life cycle assessment of microalgae and fish for eicosapentaenoic acid (EPA), docosahexaenoic acid (DHA), and protein. *J Appl Phycol*. <https://doi.org/10.1007/s10811-020-02181-6>
- Schultz N, Wintersteller F (2016) Status and trends of photoautotrophic algae cultivation from the viewpoint of a glass manufacturer. Conference Proceedings. European Algae Biomass. Berlin
- Sills DL, Paramita V, Franke MJ, Johnson MC, Akabas TM, Greene CH, Tester JW (2013) Quantitative uncertainty analysis of life cycle assessment for algal biofuel production. *Environ Sci Technol* 47:687–694
- Silva AG, Carter R, Meress FLM, Correa DO, Vargas JVC, Mariano AB, Ordonez JC, Cherer MD (2015) Life cycle assessment of biomass production in microalgae compact photobioreactors. *GCB Bioenergy* 7:184–194
- Silva Benavides AM, Torzillo G, Kopecký J, Masojidek J (2013) Productivity and biochemical composition of *Phaeodactylum tricornutum* (Bacillariophyceae) cultures grown outdoors in tubular photobioreactors and open ponds. *Biomass Bioenergy* 54:115–122
- Skarka J (2012) Microalgae biomass potential in Europe: land availability as a key issue. *Tech - Theor Prax* 21:72–79
- Smetana S, Sandmann M, Rohn S, Pleissner D, Heinz V (2017) Autotrophic and heterotrophic microalgae and cyanobacteria cultivation for food and feed: life cycle assessment. *Bioresour Technol* 245:162–170
- Soratana K, Khanna V, Landis AE (2013) Re-envisioning the renewable fuel standard to minimize unintended consequences: a comparison of microalgal diesel with other biodiesels. *Appl Energy* 112:194–204
- Subramanian RS Pipe Flow Calculations (n.d.) Working paper, Department of Chemical and Biomolecular Engineering, Clarkson University, USA Potsdam, New York, USA
- Sukarni S, Hamidi N, Wardana ING (2014) Potential and properties of marine microalgae *Nannochloropsis oculata* as biomass fuel feedstock. *Int J Energy Environ Eng* 5:279–290
- Taelman SE, De Meester S, Roef L, Michiels M, Dewulf J (2013) The environmental sustainability of microalgae as feed for aquaculture: a life cycle perspective. *Bioresour Technol* 150:513–522
- Templeton DW, Laurens LML (2015) Nitrogen-to-protein conversion factors revisited for applications of microalgal biomass conversion to food, feed and fuel. *Algal Res* 11:359–367
- Tredici MR, Rodolfi L, Biondi N, Bassi N, Sampietro G (2016) Techno-economic analysis of microalgal biomass production in a 1-ha Green Wall panel (GWP®) plant. *Algal Res* 19:253–263
- Wells ML, Potin P, Craigie JS, Raven JA, Merchant SS, Helliwell KE, Smith AG, Camire ME, Brawley SH (2017) Algae as nutritional and functional food sources: revisiting our understanding. *J Appl Phycol* 949–982

- Wernet G, Bauer C, Steubing B, Reinhard J, Moreno-Ruiz E, Weidema B (2016) The ecoinvent database version 3 (part I): overview and methodology. *Int J Life Cycle Assess* 21:1218–1230
- Woertz IC, Benemann JR, Du N, Unnasch S, Mendola D, Mitchell BG, Lundquist TJ (2014) Life cycle GHG emissions from microalgal biodiesel - a CA-GREET model. *Environ Sci Technol* 48:6060–6068
- Wu W, Wang PH, Lee DJ, Chang JS (2017) Global optimization of microalgae-to-biodiesel chains with integrated cogasification combined cycle systems based on greenhouse gas emissions reductions. *Appl Energy* 197:63–82
- Yanfen L, Zehao H, Xiaoqian M (2012) Energy analysis and environmental impacts of microalgal biodiesel in China. *Energy Policy* 45:142–151
- Zaimes GG, Khanna V (2013) Microalgal biomass production pathways: evaluation of life cycle environmental impacts. *Biotechnol Biofuels* 6:1–11
- Zhukova NV, Aizdaicher NA (1995) Fatty acid composition of 15 species of marine microalgae. *Phytochemistry* 39:351–356

Publisher's note Springer Nature remains neutral with regard to jurisdictional claims in published maps and institutional affiliations.